New Journal of Physics
An Institute of Physics and Deutsche Physikalische Gesellschaft Journal

Colloidal probe study of short time local and long time reptational motion of semiflexible macromolecules in entangled networks

M A Dichtl and E Sackmann

Lehrstuhl für Biophysik E22, Technische Universität München, James-Franck-Strasse, D-85747 Garching, Germany

New Journal of Physics **1** (1999) 18.1–18.11 (http://www.njp.org/)
Received 25 March 1999; online 10 November 1999

Abstract. We introduce a new colloidal probe technique to study local and long range motions of semiflexible actin filaments along their reptation tube axis in entangled networks. Single test filaments decorated with colloidal gold and latex beads are embedded in semidilute actin networks. The chain diffusive motion is explored by measuring the mean square displacement (MSD) of the colloidal probes in direction parallel and perpendicular to the reptation tube axis for times up to 20 min. The quasistatic constraints imposed by the neighbouring chains on the test filament are characterized in terms of an effective interaction potential $V(\vec{r})$ experienced by the test chain obtained from the distribution function of the transverse bead displacements. Remarkably large fluctuations of the width of the interaction potential and thus the tube diameter are found. At short times $4 \times 10^{-3} \leq t \leq 5 \times 10^{-2}$ s the time dependencies of the MSD in both directions obey power laws $\langle \Delta x_i^2(t) \rangle \propto t^{3/4}$ showing that the chain dynamics in this time regime can be characterized as a subdiffusive process. Between 0.5 and 1 s the MSD for both directions saturates. At times $t > 1$ s the parallel MSD crosses over into a linear regime following $\langle \Delta x^2(t) \rangle \propto t^1$ which is typical for normal Brownian diffusion. In this regime chain length dependent self-diffusivities of $D_{rept} \sim 10^{-15}$–10^{-17} m^2/s are measured which compare well with the value obtained by previous rheological measurements of the terminal relaxation time.

1. Introduction

Polymerized actin (F-actin) is a prototype of a semiflexible macromolecule exhibiting unique viscoelastic properties due to the interplay of bending energy and conformational entropy [1, 2, 3, 4]. The effective spring constant of filaments embedded in networks depends sensitively on the chain orientation with respect to the local force [3] rendering the viscoelastic impedance

1367-2630/99/000018+11$30.00

a sensitive function of the filament bending stiffness. An intriguing but still open question is whether this loss of universality is essential for the biological function of the actin based cytoskeleton. Since the function and structure of the actin network in cells is controlled by a manifold of regulating proteins binding to the filaments (such as tropomyosin [5]) they could modify the filament persistence length and thus the viscoelasticity the actin based cytoskeleton.

A unique advantage of actin as a model of semiflexible polymers is that due to its large contour length the conformational dynamics and diffusion of free and entangled filaments can be visualized by microfluorescence enabling direct measurements of the bending modulus, the self diffusivity along the tube axis D_{rept} by reptation or the shear induced chain orientation [6]. This allows to correlate viscoelastic parameters with the conformational dynamics and Brownian motion of single filaments.

The frequency dependence of the viscoelastic moduli of entangled actin solutions can be astonishingly well explained in terms of a microscopic model which is based on the assumption that each chain is transiently confined to a tube of constant diameter [7, 8]. However, till now only preliminary direct experimental evidence for this model has been provided by observations of the conformational fluctuations of fluorescent labeled filaments embedded in non-labeled entangled networks [6]. These studies provided some evidence for substantial fluctuations of the tube diameter. The self diffusion coefficient of the chains measured by analyzing the Brownian motion of the chain ends was found to be several orders of magnitude larger than the value suggested by the terminal relaxation time measured by rheology [6].

In order to gain further insight into the microscopic features of the constraints imposed by neighboring chains on a test filament and to clarify the above discrepancy we established a colloidal probe technique enabling the direct observation of local motions and the long range diffusion of selected segments of single test filaments.

Phalloidin stabilized filaments to which 17 nm gold beads or 35 nm fluorescent latex beads are coupled through biotin-streptavidin linkers or antibodies are embedded into preformed semidilute actin networks. The anisotropic motion of the beads is analyzed by in-plane confocal microscopy. In contrast to microfluorescence techniques the present method allows long time measurements of the filament dynamics with 2nm resolution in the image plane and 200 nm out-of-plane resolution.

The constraints imposed on the test chain were characterized quantitatively in terms of the interaction potential $V(\vec{r})$ experienced by the labeled segments. The potential and the corresponding force constant k was obtained from measurements of the probability distribution function of the displacement of the beads in the direction parallel and perpendicular to the local axis of the filaments and making use of Boltzmann's law. The force constants experienced by the beads vary by one order of magnitude ($1 \times 10^{-8} \leq k \leq 1 \times 10^{-7}$ Jm^{-2}) showing that the tube diameter varies drastically in contrast to the assumption of the simple tube models [9, 10].

The test filament dynamics was studied by measurement of the mean square displacement (MSD) in the direction parallel and perpendicular to the tube axis between 4 ms and 20 min. At short times ($4 \times 10^{-3} \leq t \leq 5 \times 10^{-2}$ s) the MSD obeys a power law: $MSD(t) \propto t^{\alpha}$ with $\alpha = 0.75 \pm 0.06$ in both directions in excellent agreement with the recent theoretical predictions [7, 11, 12]. The $\langle \Delta x_i^2(t) \rangle$-versus-$t$ plots saturate gradually between 0.5 and 1.5 s and the saturation level of the MSD along the tube is slightly but systematically larger than in the perpendicular direction. At long times ($t > 1$ s) the MSD parallel to the tube scales linearly with time enabling measurements of the self diffusion coefficient D_{rept} of the chains along the tube. We find diffusion coefficients between 10^{-15} m^2/s and 10^{-17} m^2/s and attribute

this large variation to the dependence of D_{rept} on the chain length L_c [7] which unfortunately could not be measured simultaneously by confocal fluorescence microscopy. The average value: $D_{rept} \sim 10^{-16}\ \mathrm{m}^2/\mathrm{s}$ agrees well with the value expected from the terminal relaxation time τ_r ($D_{rept} \sim L_c^2/2\tau_r$) measured previously by rheology [13]. This is in contrast to our previous results obtained by microfluorescence studies of the diffusion of the filament ends [6] where a much smaller value of the terminal relaxation time was found.

2. Materials and methods

Actin was isolated from rabbit muscle and purified as described previously [13]. Special care was taken to remove traces of cross-linking and other actin binding proteins by an additional gel chromatography step. Biotin was coupled to polymerized actin (F-actin) according to Okabe and Hirokawa [14] in F-buffer†. Before use the filaments were depolymerized again by transfer to excess G-buffer‡.

The colloid labeled F-actin filaments were prepared by mixing biotin labeled and normal actin monomers (G-actin) at molar ratios of 1:10 or 1:50, respectively, in F-buffer. Equimolar Phalloidin was added to the solution which stabilizes the actin filaments without remarkable perturbation of chain flexibility. Red fluorescent latex beads of 35 nm diameter (from Molecular Probes, Oregon, USA) or gold beads of 17 nm diameter (from Sigma Chemie, Deisenhofen, Germany) which were functionalized with avidin/streptavidin were coupled to the partially biotinylated actin filaments by mixing a suspension of beads (10^{11}–10^{13} beads/cm^3) with the solution of test filaments. Small aliquots of these test filaments were injected into entangled non-labeled actin solution following Käs *et al* [6]. In order to visualize the test filaments contour they were simultaneously fluorescence labeled with rhodamin-phalloidin. In this case observation was only possible by videomicroscopy despite of the addition of antioxidant to the F-buffer following Käs *et al* [6].

The motion of the colloidal beads was evaluated with a confocal laser scanning microscope (Zeiss Axiovert 100 TV equipped with the confocal setup ODYSSEY XL from Noran, Middleton, WI, USA) either by using the microscopes fluorescence mode in the case of fluorescent latex beads or the reflection mode in the case of gold beads. The system allows recordings of frame size 120×160 pixel with a rate of 240 Hz. The time it takes to record an image of a section through the bead within one of these frames is $14\ \mu$s. So this is nearly three orders of magnitude faster than the time corresponding to the frame rate of 240 Hz.

The spatial resolution of this ultramicroscopic technique in all three spatial dimensions is determined by the optical point spread function (PSF) of the beads. The static PSF was separately determined (for the 488 nm line of the Argon laser) by embedding the colloidal particles in gelatine-water mixtures and by measuring the three-dimensional intensity distribution of the Airy disk. It is important to note that the PSF is not smeared out by the motion of the beads attached to actin filaments since no broadening of the PSF due to bead motion was observed. This is a consequence of the short time required to record the image of the beads ($\sim 14\ \mu$s) as noted above. For the analysis in the z-direction stacks of images were taken at distances

† F-buffer consists of 2 mM Tris(HCl), 2mM $\mathrm{MgCl_2}$, 100 mM KCl, 0.5 mM ATP, 0.2 mM $\mathrm{CaCl_2}$, 0.2 mM DTT; $p\mathrm{H} = 7.5$.

‡ G-buffer consists of 2 mM Tris(HCl), 0.2 mM ATP, 0.2 mM $\mathrm{CaCl_2}$, 0.2 mM DTT; 0.005 volume-% $\mathrm{NaN_3}$ added as antibacterial agent; $p\mathrm{H} = 7.5$.

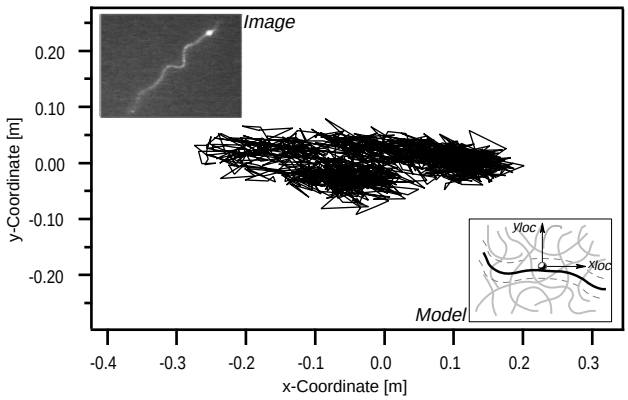

Figure 1. Plot of two dimensional trajectory of fluorescent bead coupled to fluorescent reporter filament (see insert, top left) embedded in actin network of 0.5 mg/ml (mesh size $\xi \sim 0.5\mu$m). An example of a fluorescent labeled filament is shown to visualize directly the test filament in the entangled network. Time of observation 98 s. The elongated shape of the motion defines the direction of the tube (see insert, bottom right). However, the same type of elongated diffusive motion is observed with gold beads.

of 25 nm. The half widths of the intensity distributions are $\Delta xy_{1/2} = 0.166\ \mu\text{m} \pm 1.38$ nm and $\Delta z_{1/2} = 0.334\ \mu\text{m} \pm 2.73$ nm for an iris of $D_A < 7.00$ mm. The transient bead position was obtained by determining the maximum of the three-dimensional intensity distribution for each image. For this purpose the intensity distribution of the Airy disk was fitted by a Gaussian distribution. The lateral resolution of the procedure is $\Delta xy = \pm 2$ nm in the image plane (x, y) and $\Delta z = \pm 200$ nm in the z-direction.

Since the focus in the z-direction is $0.6\ \mu$m the PSF is rather insensitive towards motions along the optical axis. This facilitates, however, the measurement of the in-plane motions since the focus has only to be readjusted very seldom once the section through the centre of the bead has been localized. The situation is different for high resolution microfluorescence microscopy since oblique motions in the vertical direction (and out of focus) could feign lateral motions (see also Discussion section).

To define the local direction of the reptation tube the motion of the gold or latex beads was followed over the whole measuring time by using a self developed image processing software which tracks the exact bead position with an accuracy of 2 nm. As shown in figure 1 elongated pathways were observed enabling to define the tube direction.

3. Results

In figures 2(*a*) and (*b*) we present typical measurements of the distribution functions $P_\perp(y)$ and $P_\parallel(y)$ of the bead displacements measured perpendicular and parallel to the tube axis respectively. For the motion perpendicular the tube orientation a well defined symmetric band is found which can be well represented by a Gaussian distribution. For the tangential direction a Gaussian distribution of similar width is found for short time displacements which goes, however, over into a constant distribution for large displacements ($\Delta x > 0.5\ \mu$m). The distributions were obtained by taking typically 7200 samples of the bead position (corresponding to a total observation time

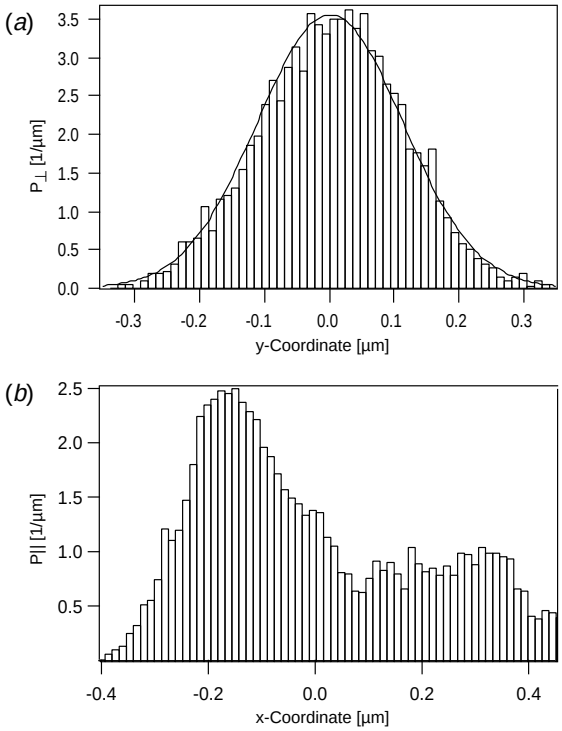

Figure 2. (*a*) Normalized distribution $P_\perp(y)$ of displacement of colloidal probe (coupled to test filament) from centre of tube in direction perpendicular to long axis (denoted as y-axis). The number of samples taken was 7200 corresponding to a measuring time of 30 s.
(*b*) Normalized distribution $P_\parallel(x)$ of the same colloidal probe (coupled to test filament) in direction along the tube axis (denoted as the x-axis) obtained with the same number of samples.

of 30 s). Histograms are plotted with a resolution of about ~ 10 nm and the maximum of $P_\perp(y)$ defines the equilibrium position.

By assuming that the entangled network is in thermal equilibrium we can interpret the transverse deflection in terms of the diffusion of the chain segment in an effective potential restricting the motion. The interaction potential limiting the perpendicular motion can then be obtained from the distribution functions $P_\perp(y)$ according to Boltzmann's law [10, 15, 16].

$$\frac{V_\perp(y)}{k_B T} = -\ln P_\perp(y) + \text{const.} \tag{1}$$

Figure 3 shows examples of several potentials $V_\perp(y)$. A surprising result is the large variability of the width of the effective interaction potential. By fitting parabola to $V_\perp(y)$ the force constants characterizing the restoring force on the filaments in the perpendicular direction is obtained as

$$k_\perp = \frac{1}{2}\frac{\partial^2}{\partial y^2} V_\perp(y). \tag{2}$$

Values of $V_\perp(y)$ and of $k_\perp$ of a selection of filaments are presented in figure 3 and in table 1, respectively. In the same way one can formally obtain apparent effective interaction potentials

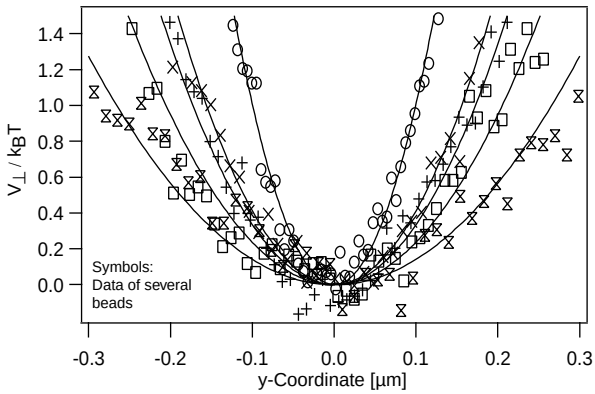

Figure 3. Effective interaction potential $V_\perp(y)$ characterizing constraint imposed by neighboring chains on motion of local chain segment in direction normal to tube axis. The associated force constants are obtained by fitting parabola (drawn lines) to the potentials $V_\perp(y)$ to $k_\perp = \frac{1}{2}\frac{\partial^2}{\partial x^2}V_\perp(y)$. Note that the plotted data refer to those given in table 1.

Table 1. Summary of effective force constants ($k_\perp$) and exponents ($\alpha_\perp$) obtained for a selection of five test chains embedded in entangled actin network of mesh size $\xi \sim 0.5\ \mu$m (actin concentration 0.5 mg/ml). The numbers in the first column correspond to the numbers of the chains in figures 2–4.

Bead number	1	2	3	4	5
$k_\perp$ (Jm^{-2})	4.77×10^{-8}	4.29×10^{-8}	1.25×10^{-8}	2.08×10^{-8}	1.09×10^{-7}
$\alpha_\perp$	0.765	0.740	0.814	0.765	0.689

$V_\parallel(x)$ and force constants $k_\parallel$ for the short time displacements along the tube axis (Dichtl M A, unpublished results of doctoral thesis, TU Munich, Germany).

In figure 4 we show double logarithmic plots of the mean square displacements of the beads parallel ($\langle\Delta x^2(t)\rangle$) and perpendicular ($\langle\Delta y^2(t)\rangle$) to the tube as function of time. In all cases the curves can be well fitted by straight lines between 4 ms and about 50 ms (see figure 4(*b*)) showing that the MSD in both directions obeys power laws $\langle\Delta x^2(t)\rangle \sim \langle\Delta y^2(t)\rangle \sim A \times t^\alpha$. Five samples evaluated in detail are presented here. The exponent varied between $0.66 \leq \alpha \leq 0.82$ but most of the exponent values lie in the range $\overline{\alpha} = 0.75 \pm 0.03$. The prefactor varied between 0.05 and $0.2\ \mu\text{m}^2/\text{s}^\alpha$ exhibiting an average value $\overline{A} = 0.1\ \mu\text{m}^2/\text{s}^\alpha$.

At longer times the MSD curves exhibit gradual slowing down for both directions. The curves saturate completely for the perpendicular direction while $\langle\Delta x^2(t)\rangle$ increases again with time after $t \geq 1$ s (see figure 4(*a*)). The asymptotic value of the MSD in the perpendicular direction is slightly but systematically smaller then along the tube axis (at the average by about 50%). The apparent and transient saturation of the MSD along the tube axis correlates well with the above mentioned finding that the probability distribution functions of small displacements in this direction $P_\parallel(x)$ exhibits a Gaussian peak of similar width as $P_\perp(y)$.

Two measurements of the long time motion ($t > 1s$) are presented in figure 5 where MSD versus time plots are shown for times up to 40 s. The complete saturation in the normal

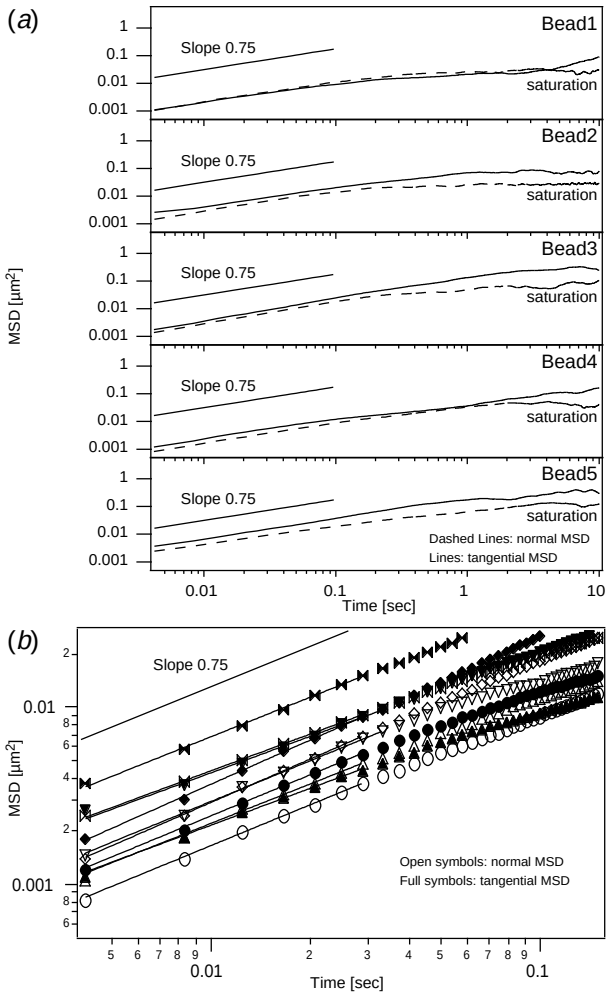

Figure 4. (*a*) Examples of double logarithmic plots of mean square displacements between 4 ms and 10 s for direction parallel (drawn lines) and perpendicular (dashed lines) to tube axis. The samples where taken by confocal microscopy with a frame rate of 240 Hz. The total measuring time was 30 s (number of samples taken: 7200). Due to statistical errors the data fluctuate strongly towards the end of the 30 s measurement time. Note that the MSD saturates between 0.5 and 1.5 s. Note also that the bead numbers in these plots refer to those in table 1

(*b*) Double logarithmic plot of the MSD data at higher resolution: between 4 and 100 ms. The MSD parallel to the tube axis is marked by full symbols and in the perpendicular direction by open symbols. A straight line is fitted to all curves between 4 and 30 ms. The results of these fits are shown in table 1.

direction is more clearly visible. Secondly it is seen that the tangential MSD exhibits a power law $\langle \Delta x^2(t) \rangle \sim 2D \times t^{\alpha}$ with $\alpha = 1$. The diffusion coefficient D obtained from the slope of the straight line is attributed to the self diffusivity D_{rept} of the filaments along the tube. By analyzing eight filaments we found values of D_{rept} between 10^{-15} and $10^{-17}\ \mathrm{m}^2/\mathrm{s}$. This large variability of the long time diffusivities points to a strong length dependence of D_{rept}. Unfortunately, the chain

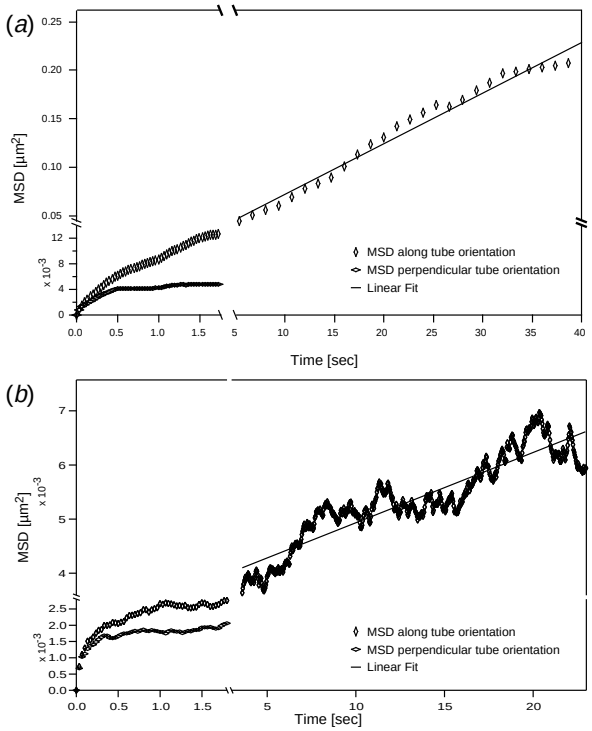

Figure 5. Two typical long time measurements of mean square displacement (MSD) $\langle \Delta x^2(t) \rangle$ of gold bead coupled to filament in direction perpendicular and parallel to tube axis.
The total measuring time was 10 min (*a*) and 2 min (*b*) but only the first 40 s (*a*) and 20 s (*b*) are shown. Note that the scales on the abscissa are different for short time scales ($t < 2$ s) and long time scales ($t > 5$ s). The slope of the straight line regime $MSD \propto t^1$ for the MSD parallel to the tube axis is constant for $1s \leq t \leq 10$ min (*a*) and $1s \leq t \leq 30$ s (*b*). The diffusion coefficients are $D_{rept} \sim 2.9 \times 10^{-15}$ m^2/s (*a*) and $D_{rept} \sim 1.9 \times 10^{-16}$ m^2/s (*b*). Note that the total root mean square displacement along the reptation tube within the total measurement time of 10 minutes is about 2 μm.
The apparent larger noise of the MSD in (*b*) is due to the smaller time intervals chosen for the evaluation of the MSD and the shorter total measuring time.

length of the test filaments could not be measured simultaneously since fluorescence labelled actin filaments bleach rapidly during the observation by laser scanning microfluorescence. From the analysis of numerous test tubes by normal videomicroscopy we know that the chain length varies between 5 μm and 40 μm and are at the average 20 μm long.

We finally measured the variation of the average force constant $k_\perp$ as a function of actin concentration for concentrations ranging from $c = 0.2$ mg/ml to 0.9 mg/ml (corresponding to mesh sizes of 0.3–0.9 μm). $k_\perp$ decreases with the square root of the concentration. Since $k_\perp$ is a measure for the width of the interaction potential (and thus for the tube width) this observation correlates well with the experimental observation that the mesh size decreases with the square root of actin concentration c. Due to the large variability of the force constants along the tube the power law cannot be determined more accurately.

4. Discussion

The colloidal probe technique provides a valuable tool to study the anisotropic motion of local segments of semiflexible macromolecules on short and long time scales and to characterize the constraints imposed by neighboring chains on a test tube in terms of a local effective potential.

By using gold and latex beads the local motion of the probe can be tracked with high spatial resolution in the image plane since the point spread function is well defined. Moreover, the confocal microscopy technique used in the present work allows high time resolutions (~ 4 ms). It should be noted that our efforts to perform LSCM measurements of the filament length by fluorescence labeling failed for two reasons. Long time measurements are impeded by bleaching effects and the instability of fluorescent labeled actin filaments under the short wavelength excitation required for fluorescence microscopy. The short time measurements yield erroneous results due to the lower time resolution (40 ms). Another possible reason is the small field-of-depth since diffusive motions in the vertical direction may feign apparent lateral motions.

A surprising result is the large variability of the tube width reflected by variation of the force constants between $1\times10^{-8} \leq k_\perp \leq 1\times10^{-7}\ \mathrm{Jm}^{-2}$. This direct observation of the tube diameter confirms previous observations of the tube width fluctuations revealed by the measurement of conformational fluctuations of fluorescent test filaments [6]. This result suggests that the simple tube model based on the assumption of constant tube diameter is too simple. The fluctuations render single filament studies more laborious since many measurements must be performed to obtain reliable distributions of physical parameters. Thus measurements of the force constant as a function of actin concentration showed that the mean value of $k_\perp$ decreases with the square root of the actin concentration but the exponent could only be measured with an accuracy of about 25% (Dichtl M A, unpublished results of doctoral thesis, TU Munich, Germany).

The scaling law found for the mean square displacement on short time scales $4\times10^{-3} \leq t \leq 5\times10^{-2}$ s: $\langle\Delta x^2(t)\rangle \propto \langle\Delta y^2(t)\rangle \propto t^{0.75\pm0.03}$ agrees well with the behaviour predicted by Gittes, Mackintosh [12] and Morse [7] for the high frequency viscoelastic response of entangled solutions of semiflexible macromolecules. These predictions are based on the assumption that at short times the elastic stress is determined by the tangential tension generated by short wavelength bending excitations of the filaments. All modes with wavelength smaller than the so-called entanglement length L_e (deflection length [4]) contribute to this tension dominated regime where the entanglement length is related to the tube width (or mesh size ξ) according to $L_e^3 = \xi^2 \times L_p$ [2]. The relaxation time of the tangential elastic stress is determined by the time scale required for the filaments to slide along the tube by diffusive motion. The relaxation modulus $G'(t)$ and the mean square displacements in the parallel tube direction should thus exhibit the same temporal scaling behaviour. This $t^{3/4}$ power law has also been reported for the subdiffusive thermal motion of beads with diameter larger than the mesh size and has been attributed to the fact that the MSD of the beads is determined by the displacement of surrounding filaments [17]. Molecular dynamics simulations of the single chain motion by Mackintosh and co-workers also showed that the mean square displacements exhibit the same power laws in the tangential and normal direction [11]. The tension dominated behaviour can only hold for times smaller than the relaxation time of the mode of wavelength L_e

$$\tau_e = \frac{\zeta L_e^4}{k_B T L_p} \tag{3}$$

where $\zeta \sim 4\pi\eta/\ln(L_e/a)$ (η viscosity of water, a diameter of actin filament). For the mesh size of the present experiment ($\xi \sim 0.5\ \mu$m) the entanglement length is $L_e \sim 1\ \mu$m and since

$L_p \sim 15$ μm the $t^{3/4}$ law is inspected to hold up to $\tau = 0.03$ s in good agreement with our experimental observation (cf figure 4(*b*)).

Following Isambert and Maggs [2] the situation changes for excitations of wavelength larger L_e and becomes dominated by the conformational dynamics of the tube. The MSD should be slowing down drastically in this regime which is expected to hold for times larger than

$$\tau_T = \frac{\zeta \xi^{16/5}}{k_B T L_p^{1/5}}. \tag{4}$$

For our experimental situation $\tau_T \sim 0.4$ s. Figure 4 shows indeed that the mean square displacements start to saturate at this time scale.

A remarkable finding is that the mean square displacements in the short time regime ($t < \tau_e$) in the two directions are nearly equal.

An important new result of the present work is the remarkably small long time diffusivity of the filaments along the tube axis. It is by two orders of magnitude smaller than the values found previously by analysis of the Brownian motion of the chain ends by the microfluorescence technique [6]. On the other side the average value of $D_{rept} \sim 10^{-16}$ m^2/s obtained in our experiment correspond to a reptation time $\tau_D = L_c^2/2D_{rept} \sim 10^6$ s for the average contour length of $L_c \sim 20$ μm. This value agrees reasonably well with the terminal relaxation time of entangled actin solutions measured by torsional rheometry ($\sim 10^5$ s; according to [13]), in contrast to the result obtained by the previous microfluorescence measurements of the chain end diffusion [6]. This result shows that the measuring time enabled by the microfluorescence technique at present is too short to yield reliable values of the filament self-diffusivity.

Inspection of a large number of fluorescence labeled actin filaments embedded in non-labeled entangled networks showed that the majority of chain lengths vary between 4 and 40μm. The large range of D_{rept}-values obtained (10^{-17}–10^{-15} m^2/s) thus demonstrates that the reptation diffusion coefficient is strongly chain-length dependent. Unfortunately the correct power law could not be determined yet. By assuming that the range of values of D_{rept} corresponds to the range of measured chain lengths (4 to 40 μm) D_{rept} would scale as $D_{rept} \propto L_c^{-2.5\pm0.5}$. This scaling law differs from the linear behaviour predicted by the simple tube model [7] for semiflexible chains. A further discrepancy with theoretical predictions is found for the frictional coefficient obtained by Einstein's law: $\zeta = k_B T/D_{rept}$. ζ is related to the solvent viscosity η_S in the tube model by $\zeta = 2\pi\eta_S L/\ln(\Lambda/a)$ where Λ is the hydrodynamic screening length which is of the order of the mesh size (~ 1 μm) and a is the filament diameter (~ 10 nm). For $D_{rept} \sim 10^{-16}$ m^2/s and $L \sim 10$ μm one obtains $\eta_S \sim 0.01$ Pa s, which is by an order of magnitude larger than the water viscosity.

The same discrepancy was recently found by rheometry by comparision of measured viscoelastic impedance spectra with spectra calculated on the basis of the tube model [7]. The solvent viscosity obtained from this comparison is again $\eta_S \sim 0.01$ Pa s (Hinner and Sackmann, unpublished results and Morse, private communication). This deviation of our experimental results from the predictions of the classical tube model could be explained in terms of transient crosslinking or local attachments of the actin filaments. Some evidence for this interpretation comes from our finding of very narrow potentials $V(\vec{r})$ (cf figure 3). If a fixed probability for the transient attachments of neighboring filaments exists one would expect both a larger frictional coefficient and a stronger length dependence of D_{rept} than predicted by the tube model.

Acknowledgments

Most helpful discussions with Erwin Frey, Fred Mackintosh, D Morse, Klaus Kroy and Jan Wilhelm are greatfully acknowledged. The work was supported by the Deutscheabstrct Forschungsgemeinschaft (SFB 413) and by the Fonds der Chemischen Industrie.

References

[1] Mackintosh F C, Käs J and Janmey P A 1996 *Biophys. J.* **20** A135
Gittes F, Schnurr B, Olmsted P D, Mackintosh F C and Schmidt C F 1997 *Phys. Rev. Lett.* **79** 3286
[2] Isambert H and Maggs A C 1996 *Macromol.* **29** 1036
[3] Kroy K and Frey E 1996 *Phys. Rev. Lett.* **77** 306
[4] Odijk T 1983 *Macromol.* **16** 1340
[5] Götter R, Kroy K, Frey E, Bärmann M and Sackmann E 1996 *Macromol.* **29** 30
[6] Käs J, Strey H, Tang J X, Finger D, Ezzel R, Sackmann E and Janmey P A 1996 *Biophys. J.* **70** 609
Käs J, Strey H and Sackmann E *Nature* **368** 226
[7] Morse D C 1998 *Macromol.* **31** 7030
Morse D C 1998 *Macromol.* **31** 7044
[8] Everaers *et al* R 1999 *Phys. Rev. Lett.* **18** 3171
[9] deGennes P G 1979 *Scaling Concepts in Polymer Physics* (New York: Cornell University Press)
[10] Doi M and Edwards S F 1979 *The Theory of Polymer Physics* (Oxford: Clarendon)
[11] Mackintosh F C *Molecular Dynamics Simulations of Single Semiflexible Chain Dynamics* unpublished
Kroy K *Viscoelasticity of Semiflexible Polymer Solutions* unpublished
Hinner B, Tempel M, Sackmann E, Kroy K and Frey E 1998 *Phys. Rev. Lett.* **81** 2614
[12] Gittes F and Mackintosh F C 1998 *Phys. Rev.* E **58** R1241
[13] Ruddies R, Goldmann W H, Isenberg G and Sackmann E 1993 *Eur. Biophys. J.* **22** 309
[14] Okabe S and Hirokawa N 1998 *J. Cell Biol.* **109** 1581
[15] Rädler J and Sackmann E 1993 *J. Phys. II France* **3** 727
[16] Jensenius H and Zocchi G 1997 *Phys. Rev. Lett.* **79** 5030
[17] Amblard F *et al* 1996 *Phys. Rev. Lett.* **77** 4470